



## Involvement of mTOR kinase in cytokine dependent microglial activation and cell proliferation

Cinzia Dello Russo, Lucia Lisi, Giuseppe Tringali, Pierluigi Navarra

### ► To cite this version:

Cinzia Dello Russo, Lucia Lisi, Giuseppe Tringali, Pierluigi Navarra. Involvement of mTOR kinase in cytokine dependent microglial activation and cell proliferation. *Biochemical Pharmacology*, Elsevier, 2009, 78 (9), pp.1242. 10.1016/j.bcp.2009.06.097 . hal-00519082

**HAL Id: hal-00519082**

**<https://hal.archives-ouvertes.fr/hal-00519082>**

Submitted on 18 Sep 2010

**HAL** is a multi-disciplinary open access archive for the deposit and dissemination of scientific research documents, whether they are published or not. The documents may come from teaching and research institutions in France or abroad, or from public or private research centers.

L'archive ouverte pluridisciplinaire **HAL**, est destinée au dépôt et à la diffusion de documents scientifiques de niveau recherche, publiés ou non, émanant des établissements d'enseignement et de recherche français ou étrangers, des laboratoires publics ou privés.

## Accepted Manuscript

Title: Involvement of mTOR kinase in cytokine dependent microglial activation and cell proliferation

Authors: Cinzia Dello Russo, Lucia Lisi, Giuseppe Tringali, Pierluigi Navarra



PII: S0006-2952(09)00568-1  
DOI: doi:10.1016/j.bcp.2009.06.097  
Reference: BCP 10245

To appear in: *BCP*

Received date: 22-5-2009  
Revised date: 19-6-2009  
Accepted date: 22-6-2009

Please cite this article as: Russo CD, Lisi L, Tringali G, Involvement of mTOR kinase in cytokine dependent microglial activation and cell proliferation, *Biochemical Pharmacology* (2008), doi:10.1016/j.bcp.2009.06.097

This is a PDF file of an unedited manuscript that has been accepted for publication. As a service to our customers we are providing this early version of the manuscript. The manuscript will undergo copyediting, typesetting, and review of the resulting proof before it is published in its final form. Please note that during the production process errors may be discovered which could affect the content, and all legal disclaimers that apply to the journal pertain.

**Involvement of mTOR kinase in cytokine dependent microglial activation and cell proliferation.**

Cinzia DELLO RUSSO<sup>1</sup>, Lucia LISI<sup>1</sup>, Giuseppe TRINGALI, and Pierluigi NAVARRA\*.

Institute of Pharmacology, Catholic University Medical School, Rome

CDR: [cinzia.dellorusso@rm.unicatt.it](mailto:cinzia.dellorusso@rm.unicatt.it)

LL: [lisilucia@virgilio.it](mailto:lisilucia@virgilio.it)

GT: [gtringali@rm.unicatt.it](mailto:gtringali@rm.unicatt.it)

PN: [pnavarra@rm.unicatt.it](mailto:pnavarra@rm.unicatt.it)

<sup>1</sup>: These authors equally contributed to this paper.

\* To whom the correspondence should be addressed:

Pierluigi Navarra

Institute of Pharmacology

Catholic University Medical School

L.go F. Vito 1

00168 Rome – Italy

Tel: +39-0630154367

Fax: +39-063050159

email: [pnavarra@rm.unicatt.it](mailto:pnavarra@rm.unicatt.it)

## Abstract

Neuroinflammation plays a prominent role in the pathophysiology of several neurodegenerative disorders, including Multiple Sclerosis. Reactive microglial cells are always found in areas of active demyelination as well as in normal appearing white matter. Microglia contribute to initiating and maintaining brain inflammation, and once activated release proinflammatory mediators potentially cytotoxic, like nitric oxide (NO). It is now evident that the mTOR signaling pathway regulates different functions in the innate immune system, contributing to macrophage activation. More recently, mTOR has been found to enhance the survival of EOC2 microglia during oxygen-glucose deprivation and increase NO synthase 2 (NOS2) expression during hypoxia in BV2 microglial cell line, thus suggesting an involvement in microglial proinflammatory activation. In the present study, we detected mTOR activation in response to two different stimuli, namely LPS and a mixture of cytokines, in primary cultures of rat cortical microglia. Moreover, mTOR inhibitors reduced NOS activity and NOS2 expression induced by cytokines, but not those induced by LPS. The mTOR inhibitor RAD001, in combination with cytokines, also reduced microglial proliferation and the intracellular levels of cyclooxygenase. Under basal conditions mTOR inhibition significantly reduced microglial viability. Interestingly, mTOR inhibitors did not display any relevant effect on astrocyte NOS2 activity or cell viability. In conclusion, mTOR selectively controls microglial activation in response to proinflammatory cytokines and appears to play a crucial role in microglial viability; thus these drugs may be a useful pharmacological tool to reduce neuroinflammation.

## Keywords

microglia, astrocytes, mTOR, NOS2, COX, cytokines

## 1. Introduction

Neuroinflammation, a process mainly sustained by activated microglial cells, plays a prominent role in the pathophysiology of several neurodegenerative disorders, including Multiple Sclerosis (MS) [1]. Lymphocytes, myeloid and reactive microglial cells are always found in areas of active demyelination in MS brains [2]; more important, activated parenchymal microglia are early detected in regions of normal-appearing white matter [3]. Microglia contribute to initiating and maintaining brain inflammation, and once activated release proinflammatory mediators potentially cytotoxic, such as nitric oxide (NO). When NO is produced in excessive amounts and for prolonged times, as it occurs by up-regulation of the inducible NO synthase isoform (NOS2), it can be neurotoxic [4]. Aberrant NOS2 induction has been found in MS and its animal model, i.e. the experimental autoimmune encephalomyelitis (EAE) [5]. Consistent with this finding, NOS2 inhibitors [6] and NO scavengers [7], as well as antisense oligonucleotides injected intraventricularly to selectively block NOS2 in the CNS [8], suppress the clinical development of EAE. In contrast, the complete inhibition of NOS2, as it occurs in NOS2 null mice, worsens the clinical course of EAE [9], suggesting that NO, up to certain levels, may be beneficial. NO is needed to induce T cell apoptosis [10], thereby contributing to the resolution of neuroinflammatory processes; moreover, phagocytosis of

1  
2  
3 apoptotic T cells by activated microglia down-regulates their pro-inflammatory functions  
4  
5 [11]. It has been shown that some of these mechanisms are defective in MS patients [12],  
6  
7 thus a partial pharmacological knockdown of NOS2 might result in beneficial effects.  
8  
9

10  
11  
12 The so-called mammalian target of rapamycin (mTOR) is a serin/threonin protein kinase  
13  
14 with a central role in the regulation of cell growth and proliferation, as well as of  
15  
16 physiological processes such as transcription, mRNA turnover and translation, ribosomal  
17  
18 biogenesis, vesicular trafficking, autophagy and cytoskeletal organization [13]. In the  
19  
20 immune system, mTOR is essential for the proper activation and proliferation of effector  
21  
22 T cells, but the development of regulatory T cells is restrained [14, 15]. Second  
23  
24 generation immunosuppressants, rapamycin (RAPA) and RAD001 (RAD) potentially block  
25  
26 cytokine-driven T cell proliferation by inhibiting mTOR kinase activity [16]. While able  
27  
28 to block T cell proliferation induced by several cytokines (including IL-1, IL-2, IL-3, IL-  
29  
30 12 and IL-15) and alloantigens [17], it appears relevant to MS that mTOR inhibitors do  
31  
32 not interfere with the ability of CD4<sup>+</sup>-CD25<sup>+</sup> regulatory T cells to induce immunological  
33  
34 tolerance [18].  
35  
36  
37  
38  
39  
40  
41  
42

43 It is now apparent that mTOR plays a crucial role in the regulation of the innate immune  
44  
45 system [19]. In freshly isolated human monocytes and primary myeloid dendritic cells  
46  
47 (DCs), mTOR activation inhibits the production of pro-inflammatory cytokines (IL-12,  
48  
49 IL-23, TNF $\alpha$  and IL-6) while it enhances the release of the antinflammatory cytokine IL-  
50  
51 10 by blocking NF $\kappa$ B activation and increasing STAT3 activity [20]. Thus, the mTOR  
52  
53 pathway might have opposite roles in the immune system [21], being necessary for T cell  
54  
55  
56  
57  
58  
59  
60  
61  
62  
63  
64  
65

proliferation and the adaptive immune responses yet critical in the down-regulation of innate immune functions. Other studies showed that mTOR inhibition decreases the global inflammatory response of in vitro generated DCs [22, 23] and reduces the production of NO by LPS-stimulated macrophages [24]. Schimtz. and coll. [25] showed that mTOR is activated following toll-like receptor stimulation by different ligands, both in human and mouse myeloid cells, leading to an increase in IL-12 and a decrease in IL-10 production, as also shown by Weichhart and coll. [20]. While IL-12 was increased, other proinflammatory markers (such as  $\text{TNF}\alpha$ , IL6 and NO) were reduced by RAPA [25]. Therefore, further studies to elucidate the exact role of mTOR in the innate immune system are needed, even though the relevance of this pathway in the regulation of monocyte-macrophage functions is undisputed at present.

Looking at the central nervous system resident macrophages, i.e. microglial cells, it has been demonstrated that mTOR enhances the survival of EOC2 microglial cells during oxygen-glucose deprivation [26] and mediates NOS2 induction during hypoxia in the BV2 microglial cell line [27], suggesting a role in the control of microglial functions. We tested this hypothesis in primary cultures of rat cortical microglia activated in vitro by two different stimuli: the bacterial endotoxin (lipopolysaccharide, LPS) and a more relevant stimulus to MS patho-physiology, i.e. a mixture of the pro-inflammatory cytokines interleukin- $1\beta$  (IL- $1\beta$ ), tumor necrosis factor  $\alpha$  ( $\text{TNF}\alpha$ ) and interferon  $\gamma$  ( $\text{IFN}\gamma$ ), altogether referred to as TII. The activation of mTOR (measured by phosphorylation of the protein at ser 2448) [28] could be detected after 2 h of stimulation with both stimuli. The pharmacological inhibition of mTOR was able to reduce cytokine-dependent NOS2

activity and expression, but had not effect on LPS-induced NOS activity. Subsequently, we tested the effect of mTOR inhibition on cyclooxygenase (COX) expression and activity, taken as additional parameters of microglial activation. The cytokine mixture increased COX gene expression and activity, the latter measured through the assessment of prostaglandin E2 (PGE2) release in the incubation medium after 48 h of incubation. The addition of RAD antagonized cytokine-induced COX expression and tended to reduce PGE2 production, albeit reduction did not attain statistical significance. The overall inhibitory effects of mTOR blockers were not due to increased microglial toxicity, as shown by the MTS reduction assay. However, mTOR inhibitors reduced microglial proliferation and under basal conditions also cell viability. Both inhibitors had no significant effects on astrocyte NOS2 activity and cell viability. Taken together, these findings indicate that mTOR is crucial for microglial proliferation and their activation in response to pro-inflammatory cytokines, thus providing pre-clinical evidence for a possible clinical exploitation of mTOR inhibitors in the treatment of MS and other inflammatory-based CNS pathologies.

## 2. Methods

### 2.1 Materials

Cell culture reagents [Dulbecco's modified Eagle's medium (DMEM), DMEM-F12 and Fetal calf serum (FCS)] were from Invitrogen Corporation (Paisley, Scotland).

Antibiotics were from Biochrom AG (Berlin, Germany). Bacterial endotoxin LPS (*Salmonella typhimurium*) was from Sigma Aldrich (St Louis, MO, USA). Recombinant



proinflammatory cytokines, namely human tumor necrosis factor- $\alpha$  (TNF $\alpha$ ), human interleukin-1 $\beta$  (IL-1 $\beta$ ) and rat interferon- $\gamma$  (IFN $\gamma$ ) were purchased from Endogen (Pierce Biotechnology, Rockford, IL, USA). The mTOR inhibitor, RAD001 (RAD), was kindly provided by Novartis Pharmaceutical (Basel, Switzerland), while rapamycin (RAPA) was purchased from Tocris Bioscience (Bristol, UK). COX1 and COX2 rabbit polyclonal antibodies were from Cayman (Ann Arbor, Michigan, USA);  $\beta$ -actin (clone AC-74) mouse monoclonal antibody was from Sigma Aldrich; and rabbit polyclonal anti-phospho [Ser2448] mTOR was purchased from Novus Biological (Littleton, CO, USA).

## 2.2 Cell cultures

Primary enriched cultures of rat microglia were prepared from mixed cultures of cortical glial cells (at in vitro day 14), as described previously [29]. Briefly, microglial cells were detached from the astrocyte monolayer by gentle shaking. The cells were plated in 96-well plates at a density of  $3 \times 10^5$  cells/cm<sup>2</sup> using 100  $\mu$ L/well DMEM-F12 containing 10% FCS and antibiotics. Under these conditions, the cultures were 95-98% CD11b positive. Experiments were carried out in the same medium used for cell plating to reduce microglial death, which normally occurs after splitting from astrocytes [30]. Microglial activation was induced by incubating cells with pro-inflammatory cytokines (10 UI/ml IFN $\gamma$ , 10 ng/ml TNF $\alpha$  and 10 ng/ml IL-1 $\beta$ ) or 1 ng/ml LPS for different times as indicated in figure legend. At the end of each experiment, the incubation medium was collected and used for the measurement of NO production or PGE2 release.

Primary cultures of cortical rat astrocytes were obtained as we previously described [30]. Briefly, after dissecting and digesting the cortices, cells were plated in 75-cm<sup>2</sup> flasks (1 brain/flask). The culture medium was changed within 24 h, and then twice a week until the astrocytes were grown to form a monolayer. At this time, the culture medium was replaced with PBS-without Ca<sup>++</sup> and Mg<sup>++</sup> (Sigma Aldrich) and the flasks were vigorously shaken to remove non adherent cells, oligodendrocytes and microglia. Subsequently, astrocytes were detached from the flask by a 5-min 0.05% trypsin-EDTA treatment (Biochrom Ltd, UK). Astrocytes obtained with this procedure were then subcultured twice, the first time in 75-cm<sup>2</sup> flasks and the second time directly in multiwell plates used for the experimental procedures, carried out in 1% FCS DMEM.

### 2.3 Nitrite assay

NOS2 activity was assessed indirectly by measuring nitrite accumulation in the incubation media [31]. Briefly, an aliquot of the cell culture media (80 µL) was mixed with 40 µL Griess Reagent (Sigma Aldrich) and the absorbance measured at 550 nm in a spectrophotometric microplate reader (Perkin Elmer Inc., MA, USA). A standard curve was generated during each assay in the range of concentrations 0-100 µM using NaNO<sub>2</sub> (Sigma Aldrich) as standard. In this range, standard detection resulted linear and the minimum detectable concentration of NaNO<sub>2</sub> was  $\geq 6.25$  µM. In the absence of stimuli, basal levels of nitrites were below the detection limit of the assay after 24 h incubation.

### 2.4 Cell Viability measurement

At the end of each experiment, microglial viability was assessed by reduction of the tetrazolium compound (3-(4,5-dimethylthiazol-2-yl)-5-(4-sulphophenyl)-2H-tetrazolium, inner salt; MTS) contained in the CellTiter Aqueous One Solution Reagent (Promega, Madison, WI, USA). For this assay cells were seeded in 96 well plates. At the end of the experimental procedure, 20  $\mu$ l of MTS reagent were added to the cells that were further incubated for 2 h. Living cells bio-reduces yellow MTS into a purple soluble formazan product with an absorbance peak at 492 nm, that was read in a spectrophotometer plate reader.

## 2.5 Cell proliferation assay

Microglial proliferation rate was determined using a non-radioactive proliferation assay (Exalpha Biological Inc., Maynard, MA, USA), used according to the manufacturer's instructions. This ELISA assay measures the incorporation of 5-bromo-2-deoxyuridine (BrdU) into newly synthesized DNA of actively proliferating cells. Microglial cells were incubated in plain medium or medium containing different testing substances for 24 h. BrdU solution was added 8 h later directly in the incubation medium, and cells were kept in the incubator for the remaining 16 h. At the end of the incubation time, medium was removed and cells were fixed. BrdU immunoreactivity was measured using a specific primary antibody provided by the kit. Control wells that were not exposed to BrdU, were processed in the same way as experimental samples and were used as background for the assay. Absorbance was read at 450 nm and 540 nm. Total net OD was calculated per each sample ( $OD_{450} - OD_{540}$  without values measured for background samples). Data are

expressed as percentage of Control values. The sensitivity of BrdU incorporation is comparable to standard radioactive [ $^3\text{H}$ ]-thymidine incorporation assays.

## 2.6 PGE2 radioimmunoassay

PGE2 was measured by RIA as previously described in detail [32]. Incubation mixtures of 1.5 ml were prepared in disposable plastic tubes. Culture derived media samples (250  $\mu\text{l}$ ) were mixed with [ $^3\text{H}$ ]PGE2 (GE Healthcare, Little Chalfont, UK) (2,500-3,000 cpm) in 0.025 M phosphate buffer (pH 7.5). Antiserum reactive against PGE2 (kindly provided by Prof. G. Ciabattini) was added with sufficient phosphate buffer to achieve a final dilution of 1:120,000 in a total incubation volume of 1.5 ml. A standard curve was generated with duplicate aliquots of PGE2 at 2-400 pg/tube. After 24 h, free PGE2 was removed with activated charcoal (Sigma Aldrich). Supernatants (containing antibody-bound PGE2) were combined with 10 ml liquid scintillation fluid, and radioactivity was measured by liquid scintillation counting (Perkin Elmer Inc.). The detection limit of the assay was 2 pg/tube and the  $\text{EC}_{50}$  40 pg/tube. The intra- and inter-assay variability was 5 and 10% respectively.

## 2.7 mRNA analysis in real time PCR

Total cytoplasmic RNA was extracted using the RNeasy®Micro kit (Qiagen, Hilden, Germany), which included a 15 min DNase treatment. RNA concentration was measured using the Quant-iT™ RiboGreen® RNA Assay Kit (Invitrogen Corporation). A standard curve in the range of 0-100 ng was run in each assay using 16S and 23S ribosomal RNA (rRNA) from *E. coli* as standard and provided by the kit. Aliquots (0.5  $\mu\text{g}$ ) of RNA were

converted to cDNA using random hexamer primers. Quantitative changes in mRNA levels were estimated by real time PCR (Q-PCR) using the following cycling conditions: 35 cycles of denaturation at 95°C for 20 sec; annealing at 59°C for 30 sec; and extension at 72°C for 30 sec; using the Brilliant SYBR Green QPCR Master Mix 2X (Stratagene, La Jolla, CA, USA). PCR reactions were carried out in a 20 µL reaction volume in a MX3000P real time PCR machine (Stratagene). The primers used for NOS2 detection were: 1704F (5'-CTG CAT GGA ACA GTA TAA GGC AAA C-3'), and 1933R (5'-CAG ACA GTT TCT GGT CGA TGT CAT GA-3'), which yield a 230 base pair (bp) product. The primers used for COX1 detection were 154F (5'- CCT CAC CAG TCA ATC CCT GT-3'), and 384R (5'-AGG TGG CAT TCA CAA ACT CC-3'), which yield a 231bp product; the primers used for COX2 detection were 677F (5'-GCA TTC TTT GCC CAG CAC TTC ACT-3'), and 774R (5'-TTT AAG TCC ACT CCA TGG CCC AGT-3') which yield a 98bp product. The primers used for  $\alpha$ -tubulin were: F984 (5'-CCC TCG CCA TGG TAA ATA CAT-3'), and 1093R (5'- ACT GGA TGG TAC GCT TGG TCT-3'), which yield a 110 bp product. Relative mRNA concentrations were calculated from the take-off point of reactions (threshold cycle, Ct) using the comparative quantitation method performed by Stratagene software and based upon the  $-\Delta\Delta C_t$  method [33]. This analysis approximates a given sample's target mRNA (e.g., NOS2) level relative to the mean of the target mRNA levels in untreated controls ("calibrator" value), thus permitting statistical analysis of deviation from the mean even among the controls. Ct values for  $\alpha$ -tubulin expression served as a normalizing signal. In each assay, the PCR efficiency was also calculated using serial dilution of one experimental sample; efficiency values between 94-98% were found for each primer set and taken into account

for the comparative quantitation analysis. At the end of Q-PCR, the products were separated by electrophoresis through 2% agarose gels containing 0.1 µg/ml ethidium bromide to ensure the product was the correct size.

## 2.8 Western immunoblot

Microglia were lysed in RIPA buffer (1mM EDTA, 150 mM NaCl, 1% igeal, 0.1% SDS, 0.5% sodium deoxycholate, 50 mM Tris-HCl, pH 8.0) (Sigma Aldrich) containing protease inhibitor cocktail diluted 1:250 (Sigma Aldrich) ( $1 \times 10^6$  cells/100µl RIPA). The protein content in each sample was determined by Bradford's method (Biorad, Hercules, CA, USA) using bovine serum albumin as standard. A 20-µg aliquot of protein was mixed either 1:2 with 2X Laemmli Buffer (Biorad) or 1:3 with 3X gel sample buffer (150 mM Tris-HCl pH 6.8, 7.5% SDS, 45% glycerol, 7.5% of bromophenol blue, 15% β-mercaptoethanol) depending on protein content, boiled for 5 min, and separated through 10% polyacrylamide SDS gels. Apparent molecular weights were estimated by comparison to colored molecular weight markers (Sigma Aldrich). After electrophoresis, proteins were transferred to polyvinylidene difluoride membranes by semi-dry electrophoretic transfer (Biorad). The membranes were blocked with 10% (w/v) low-fat milk in TBST (10 mM Tris, 150 mM NaCl, 0.1% Tween-20, pH 7.6) (Biorad) for 1 h at room temperature, and incubated in the presence of the primary antibody overnight with gentle shaking at 4 °C. Primary antibodies for phosphorylated mTOR, β-actin, COX1, and COX2 were used at the final concentration of 1:1000. Primary antibodies were removed, membranes washed three times in TBST, and further incubated for 1 h at room temperature in the presence of specific secondary antibody, anti-rabbit IgG-HRP (Vector

Laboratories, Burlingame, CA, USA) diluted 1:15,000-20,000 or anti-mouse IgG-HRP (Sigma Aldrich) secondary antibody, diluted 1:8000. Following three washes in TBST, bands were visualized by incubation in ECL reagents (GE Healthcare) and exposure to X-ray film (Kodak, Rochester, NY, USA). The same membranes were washed three times in TBST, blocked with 10% (w/v) low-fat milk in TBST for 1 h at room temperature and used for  $\beta$ -actin immunoblot. Band intensities were determined using ImageJ software (National Institutes of Health) from autoradiographs obtained from the minimum exposure time that allow band detection, and background intensities (determined from an equal-sized area of the film immediately above the band of interest) were subtracted.

## 2.9 Data analysis

All experiments were done using 5-6 replicates per each experimental group, and repeated at least 3 times. Duplicates were used for the RNA analysis, samples were assayed in triplicates, and the experiments were repeated at least twice. Data were analyzed by one- or two-way ANOVA followed by Bonferroni's post hoc tests; P values < 0.05 were considered significant.

## 3. Results

### 3.1 mTOR promotes cytokine dependent microglial activation

Microglial cells were activated using a mixture of proinflammatory cytokines (TII), *i.e.* 10 IU/ml IFN $\gamma$ , 10 ng/ml TNF $\alpha$ , and 10 ng/ml IL-1 $\beta$  or 1 ng/ml LPS, a widely used pro-

1  
2  
3 inflammatory stimulus that triggers a full activation of microglia [29]. Cells were  
4  
5 incubated for 2 h, and then subjected to protein analysis for mTOR phosphorylation at ser  
6  
7 2448. Both stimuli significantly augmented mTOR phosphorylation (Fig. 1A); in  
8  
9 particular, LPS increased by about 70% and TII by about 40% the amount of  
10  
11 phosphorylated mTOR normally detected under basal conditions (Fig. 1B). RAPA and its  
12  
13 analog RAD are second generation immunosuppressants that block mTOR activation; in  
14  
15 this model, 1nM RAD was able to attenuate the increase in mTOR phosphorylation at ser  
16  
17 2448 induced by TII treatment (Fig. 2).  
18  
19  
20  
21  
22  
23

24 When used in the range of 0.1-5 nM, both mTOR inhibitors counteracted the increase in  
25  
26 NO production elicited by TII (Fig. 3A-B), while having no significant effect on LPS-  
27  
28 stimulated nitrite production (Fig. 3C-D). The increased in NO production in microglia  
29  
30 cells is mediated by the up-regulation of inducible NOS isoform; the steady state levels of  
31  
32 NOS2 mRNA were almost undetectable by Q-PCR under basal conditions (average Ct ~  
33  
34 31), and increased in response to both pro-inflammatory stimuli (Fig. 4A). However, the  
35  
36 time-course effects of the two stimuli were remarkably different: LPS triggered a rapid  
37  
38 up-regulation of NOS2, with mRNA levels reaching a peak at 4 h and thereafter declining  
39  
40 with time up to 24 h, the latest time point studied. Conversely, TII caused a slower and  
41  
42 progressive increase in the NOS2 mRNA levels, with the highest amounts measured after  
43  
44 24 h. In subsequent experiments a fixed time-point at 24 h was adopted, and microglial  
45  
46 cells were stimulated in the presence of 1 nM RAD, as indicated in Fig. 4B-C. RAD  
47  
48 significantly reduced NOS2 expression induced by TII (Fig. 4B), while prevented the  
49  
50 reduction of NOS2 mRNA levels usually observed after 24 h of LPS treatment (Fig. 4C).  
51  
52  
53  
54  
55  
56  
57  
58  
59  
60  
61  
62  
63  
64  
65



As an additional parameter of microglial activation, we studied the effect of cytokines, given alone or in the presence of mTOR inhibitors, on COX gene expression and activity. The amounts of PGE2 released in the incubation media were taken as a marker of COX activity, and TII was found to significantly increase PGE2 release from microglia after 48 h incubation. In this experimental setting, the stimulatory effects of LPS are usually more rapid and marked (not shown). RAD given in the range 0.1-1 nM tended to reduce PGE2 production, albeit such reduction did not attain statistical significance (Fig. 5A). TII significantly increased the total amount of constitutive COX isoform, namely COX1 (Fig. 5B-C), while displaying a slight but not statistically significant stimulatory effects on COX2 levels (Fig. 5D-E). 1 nM RAD significantly reduced COX1 protein levels both under basal condition and after TII challenge (Fig. 5B-C).

### 3.2 mTOR controls microglial proliferation and viability

In order to exclude possible nonspecific toxic effects of mTOR inhibitors, MTS reduction was measured at the end of selected experiments. Microglia were activated with TII for 24 h, and mTOR inhibitors were added at the beginning of each experiment as indicated (Fig. 6A). TII significantly increased MTS reduction in comparison to Controls, indicating that the cytokines significantly increase cell viability. Co-incubation with 1-10 nM RAD resulted in a complete reversal of TII-stimulated MTS reduction, bringing back MTS levels to those of untreated Controls. Similar results were obtained using RAPA. Both inhibitors significantly reduced microglial cell viability with respect to Controls when used alone (Fig. 6A). In experiments looking at cell proliferation, RAD

(0.1-10 nM) reduced microglial proliferation in a significant and dose-dependent manner (Fig. 6B). Likewise, both TII (Fig 6B) and LPS (data not shown) suppressed microglial proliferation, and the addition of RAD further increased the inhibitory effect exerted by TII (Fig. 6B). The observed interference of mTOR inhibitors with microglial viability and proliferation raised the question as to whether the previous findings on NO production were somewhat influenced by the varying number of cells in the system. Therefore, the data of nitrite production were normalized by the amount of proteins relative to each treatment. As previously observed, 1nM RAD significantly inhibited nitrite production in microglial cells activated with TII (Fig. 7A) without affecting LPS stimulatory effects (Fig. 7B), thereby confirming that the effects of RAD on NOS regulation are not dependent on cell number and viability.

### 3.3 The pharmacological block of mTOR does not interfere with astrocyte function

NOS2 activity can be also induced in primary cultures of rat cortical astrocytes by LPS and cytokines [34]. However, these cells are less reactive than microglia. In fact, we detected sizable amounts of nitrites in the incubation media after 48 h challenge with TII, and the levels were roughly 2-3 fold lower than those found in microglial cultures after 24 h challenge. RAD, given in the range 0.01-10 nM, tended to reduce nitrite production in astrocytes, although such effect was not statistically significant (Fig. 8A). On the other hand, RAPA used within the same range of concentrations displayed no inhibitory effect (Fig. 8B). mTOR inhibitors did not affect astrocyte viability, either given alone or in combination with TII (Fig. 8C).

#### 4. Discussion

In the present study we detected mTOR activation associated to the pro-inflammatory activation of microglial cells in response to two different proinflammatory stimuli, namely bacterial endotoxin and a mixture of inflammatory cytokines, in this work referred to as TII. The pharmacological inhibition of mTOR was able to reduce microglial responses elicited by the cytokines, but failed to inhibit LPS-induced NOS2 activity. The mTOR inhibitors also interfered with microglial viability and proliferation. All of these effects appeared to be cell selective, since mTOR inhibitors did not affect pro-inflammatory activation and cell viability in astrocytes. These findings clearly indicate that the mTOR pathway plays a relevant role in mediating innate immune responses within the CNS, similar to the observations in peripheral cells of the immune-inflammatory lineage [19].

In fact, we detected increased levels of phosphorylated mTOR in primary cultures of microglial cells in response to both LPS and TII. Phosphorylation at ser-2448 on the mTOR protein primarily reflects a feedback signal from the mTOR downstream target, the p70 S6 kinase (p70S6K), and it is therefore considered a reliable marker of mTOR activation within the cells [28]. While both stimuli increased mTOR phosphorylation at ser-2448, the effect of LPS was more marked in comparison to TII. A higher degree of mTOR phosphorylation by LPS might probably account for the fact that the inhibition of mTOR by appropriate pharmacological tools failed to counteract LPS activation of microglia, whereas mTOR inhibitors were able to reduce TII-stimulated nitrite

production in these cells. The same results were obtained if data were normalized on the protein content relative to each treatment. Moreover, the mTOR inhibitor RAD antagonized cytokine-dependent NOS2 induction after 24 h of treatment, but further increased NOS2 mRNA levels induced by LPS, which is consistent with the lack of inhibition by RAD of NO production in LPS-activated microglia. Under inflammatory conditions, high levels of NO are generated by the up-regulation of NOS2. In microglial cultures we observed a rapid up-regulation of NOS2 after a LPS challenge, with the highest levels measured after 4 h incubation, whereas TII caused a slower and progressive increase in the NOS2 mRNA steady state levels with the highest amounts measured after 24 h, at a time when the response to LPS stimulation is declining towards baseline. These data may be reasonably explained by the recruitment of different signaling pathways by the two stimuli, and/or by a different timing in recruitment, which can account for the different effects of RAD on NOS2 activity and expression depending on the presence of one or another of the two pro-inflammatory stimuli. Interestingly, both proinflammatory [35, 36] and antiinflammatory effects [24] have been described in peripheral macrophages in association to mTOR inhibition. Most of the currently available data suggest that mTOR acts as a negative feedback regulator in LPS activated macrophages by blocking NFkB activation and thus reducing the inflammatory responses [20]. NFkB is a critical transcription factor in the regulation of NOS2 expression, and therefore mTOR might regulate NOS2 expression through an interaction with NFkB signaling pathway. In fact, both stimulatory [37] and inhibitory effects [38] on NFkB activation mediated by the mTOR pathway have been described.

1  
2  
3 RAD also reduced the stimulatory effect of TII on PGE2 production (albeit not  
4  
5 significantly) and the intracellular content of COX enzymes, thus providing further  
6  
7 support to the hypothesis that the activation of mTOR mediates cytokine-dependent  
8  
9 microglial proinflammatory responses. The findings presented in this study are consistent  
10  
11 with a large body of evidence showing that pro-inflammatory cytokines signal through  
12  
13 the activation of the mTOR pathway in several cellular systems. For example, TNF $\alpha$ -  
14  
15 dependent apoptosis in osteoclasts is mediated by mTOR activation [39]; in endothelial  
16  
17 cells, RAPA was shown to reduce IL-1 $\beta$ -dependent production of vascular endothelial  
18  
19 growth factor [40] as well as TNF $\alpha$ -evoked IL-6 release [41]. Moreover, TNF impairs  
20  
21 insulin signaling through insulin receptor substrate-1 through the activation of PI3-  
22  
23 kinase/Akt/mTOR pathway [42], as demonstrated by the fact that the effects of TNF $\alpha$   
24  
25 could be reverted by mTOR inhibitors. Recently, it has been shown that TNF $\alpha$  promotes  
26  
27 mTOR activation via the inhibitor of NF $\kappa$ B kinase  $\beta$  (IKK $\beta$ ) [43]. The latter increases  
28  
29 phosphorylation of the inhibitory protein tuberous sclerosis complex 1 (TSC1), leading to  
30  
31 the subsequent activation of mTOR complex 1 (mTORC1) [43]. In fact, mTOR exists in  
32  
33 at least two different complexes, mTORC1 and mTORC2, with distinct relationships  
34  
35 toward both upstream and downstream effectors as well as different regulations of  
36  
37 intracellular function [13]. mTORC1 is critically involved in the regulation of protein  
38  
39 translation; in fact, its two main downstream targets (the 4E binding protein1, 4EBP1,  
40  
41 and the above mentioned p70S6K) are key components of the translation machinery [44].  
42  
43 RAPA and its analogs selectively inhibit the function of mTORC1 [45]; thus, a decrease  
44  
45 in protein translation may account for the inhibitory effects observed in TII-activated  
46  
47 microglial cells, particularly the reduction on COX intracellular content, since we could  
48  
49  
50  
51  
52  
53  
54  
55  
56  
57  
58  
59  
60  
61  
62  
63  
64  
65

not observe any significant inhibition on both COX1 and COX2 mRNA levels (not shown).

In order to exclude that the inhibitory effects of RAPA and RAD were simply due to increased cell toxicity, we assessed MTS reduction in the cultures at the end of the experiments. TII increased MTS reduction in microglial cells, which is an index of augmented cell viability. mTOR inhibitors were able to bring back the stimulatory effect of TII to control levels that may be considered as another evidence of the inhibitory effects of these drugs on cytokine-dependent microglial activation. However, microglial viability was significantly affected by mTOR inhibition under baseline conditions, which is consistent with the findings that mTOR inhibition can lead to autophagic cell death [46] or to apoptosis [47]. Moreover, RAD reduced in a significant and dose-dependent manner microglial cell proliferation, assessed as the rate of BrdU incorporation into newly synthesized DNA in dividing cells. Interestingly, we observed a reduction of microglial proliferation in response to cytokine stimulation, an effect that may be due to increased production of free radicals and other toxic metabolites, and RAD further amplified this inhibitory effect. Taken together these data underlie the important role of mTOR in the regulation of microglia cell viability and proliferation. Such effects may also contribute to the neuroprotective actions of mTOR inhibitors observed in vivo in some neurological disorders. RAPA significantly ameliorates the functional recovery in mice after experimental traumatic brain injury, probably due to the reduction of microglial activation [48]. Interestingly, in this model RAPA had no significant effect on reactive astrocytes at the site of injury, which is fully consistent with our in vitro data. In fact, we

1  
2  
3 did not observe any significant reduction in cytokine-dependent NOS2 activity, nor any  
4  
5 effect on cell viability in primary cultures of rat astrocytes. Thus the effects of mTOR  
6  
7 inhibitors seem to be cell specific. Similar findings were obtained in peripheral models,  
8  
9 where RAD has been found to selectively reduce macrophage infiltration of  
10  
11 atherosclerotic plaques without affecting smooth muscle cell viability [46]. At variance  
12  
13 with the above evidence, it has been recently shown that mTOR may be involved in cell  
14  
15 growth and reactive transformation of spinal cord astrocytes, particularly in response to  
16  
17 epidermal growth factor [49].  
18  
19  
20  
21  
22  
23

24 In conclusion, in this study we demonstrated that mTOR inhibitors selectively affect  
25  
26 microglial function. The overall effects on microglia observed in this study, the fact that  
27  
28 mTOR inhibitors reduce cytokine dependent T-cell proliferation while increasing the  
29  
30 ability of regulatory T cells to induce immunological tolerance, may altogether lead to  
31  
32 envision these drugs as useful therapeutic tools to reduce neuroinflammation.  
33  
34  
35  
36  
37  
38  
39  
40

#### 41 **Acknowledgments**

42  
43 This work was supported by grants from the National Multiple Sclerosis Society and  
44  
45 from *Fondi di Ateneo* to CDR and Novartis Pharmaceutical to PN. We are very grateful  
46  
47 to Dr. W. Schuler for critical reading of the MS and useful comments throughout the  
48  
49 preparation of this work.  
50  
51  
52  
53  
54  
55  
56  
57  
58  
59  
60  
61  
62  
63  
64  
65

### Figure legends

Figure 1. Analysis of mTOR phosphorylation during microglial activation. (A) Whole-cell lysates were prepared from microglial cells incubated for 2 h in plain medium or in medium containing either TII or LPS. Equal amounts of proteins were analyzed by western blot for phosphorylated mTOR kinase (p-mTOR), upper gel. mTOR phosphorylation at ser-2448 is a marker of mTOR activation within the TORC1. The same blots were subsequently probed for  $\beta$ -actin, lower gel. (B) Quantitation of densitometry where p-mTOR values are reflected relative to those for  $\beta$ -actin. Data are expressed as mean  $\pm$  SEM of n= 2 replicates for each group, each assayed in triplicates. Representative of two different experiments. \*\*\* and \* p<0.001 and p<0.05 vs controls.

Figure 2. RAD001 reduces mTOR phosphorylation induced by TII. (A) Whole-cell lysates were prepared from microglial cells activated with TII for 2 h. 1 nM RAD was added at the beginning of the experiment and equal amounts of protein were analyzed by western blot for phosphorylated mTOR kinase (p-mTOR). (B) Quantitation of densitometry wherein p-mTOR values are reflected relative to those for  $\beta$ -actin. Data are expressed as mean  $\pm$  SEM of n= 2 replicates for each group, each assayed in triplicates. Representative of two different experiments. \*\*\* p<0.001 vs controls; §§§ P<0.001 vs TII.

Figure 3. Effects of the mTOR inhibitors on microglial NO production. Microglia were activated for 24 h with TII (A-B) or LPS (C-D). The mTOR inhibitors, RAD001 (RAD) and rapamycin (RAPA), were added to the cells in nM concentrations at the beginning of the experiments. NO production was assessed indirectly by measurement of nitrite



accumulation in the incubation medium (Griess method). Data are expressed as means  $\pm$  SEM (n=5). Results were analyzed by one-way ANOVA followed by Bonferroni's post test. \*\*\*,  $P < 0.001$  vs Controls; §§ and §§§,  $P < 0.01$  and  $< 0.001$  vs TII.

Figure 4. Effects of the mTOR inhibitor RAD001 on NOS2 expression. (A) Total cytosolic RNA was prepared from Control, or microglial cells treated with LPS or TII for different times, and used for Q-PCR analysis of NOS2 expression. Data are expressed as fold change *versus* each respective Control, taken as calibrator for comparative quantitation analysis of mRNA levels. Each sample was measured in triplicate, the experiment was repeated 2 times with similar results. Controls were equal 1, thus not reported in the graph. Both LPS and TII significantly induced NOS2 expression in comparison to Controls (two-way ANOVA). Data are Means  $\pm$  SEM. \* and \*\*\*,  $P < 0.05$  and  $0.001$  vs TII; two-way ANOVA followed by Bonferroni's post test. Microglia were incubated for 24 h with plain medium or activated with TII (B) or LPS (C). Where indicated, 1 nM RAD001 was added at the beginning of the experiment. Data are means  $\pm$  SEM. \*\*\*,  $P < 0.001$  vs Controls; §§§,  $P < 0.001$  vs TII (B) or LPS (C); one-way ANOVA followed by Bonferroni's post test.

Figure 5. Effects of the mTOR inhibitor RAD001 on COX activity and expression. (A) Microglial cells were incubated for 48 h in plain medium or medium containing TII; when indicated RAD (0.1-1 nM) was added to the cells at the beginning of the experiment. PGE2 release in the incubation media was assessed by RIA. Data are expressed as pg/ml of PGE2, and are means  $\pm$  SEM of 4 replicates per each group. The

experiment is representative of three different experiments run in the same conditions. \*,  $P < 0.05$  vs Controls. Whole-cell lysates were prepared from microglial cells treated as described above. 20  $\mu$ g of protein were analyzed by western blot for the expression of COX1 (B) and COX2 (D) enzyme. Line 1: Controls; Line 2: TII; Line 3: TII/0.1 nM RAD; line 4: TII/1 nM RAD; line 5: 1 nM RAD. TII significantly increased intracellular levels of COX1 (C) while having a slight but not significant stimulatory effect on COX2 (E). 1nM RAD significantly reduced COX1 intracellular levels, both under basal conditions and after stimulation with TII (C). \*\* and \*\*\*,  $P < 0.01$  and  $P < 0.001$  vs Controls; §,  $P < 0.05$  vs TII.

Figure 6. Effects of RAD001 on microglial viability and proliferation. (A) Possible toxicity due to pharmacological treatments was assessed by the MTS reduction assay. Microglia were activated with TII for 24 h and mTOR inhibitors were added at the beginning of each experiment as indicated. Cells were incubated with MTS for 2 h after which the absorbance was measured at 490 nm. \*\*\*,  $P < 0.001$  vs Control; §§§  $P < 0.001$  vs TII. (B) Cells were incubated in plain medium or medium containing different doses of RAD001 for 24 h. BrdU was added 8 h later directly in the incubation medium, and cells were incubated at 37 °C for the remaining 16 h. At the end of the incubation time, medium was removed and cells were fixed. BrdU immuno-reactivity was measured with a specific ELISA kit. Data are expressed as percentage of Control, and are means  $\pm$  SEM (n=5). \*\*\* and \*\*,  $P < 0.001$ , and 0.01 vs Control. §  $P < 0.05$  vs TII.

Figure 7. Effects of RAD on microglial NO production. Cells were stimulated with TII (A) or LPS (B). RAD was added at the beginning of the experiment, in the nM range as indicated. After 24h incubation, the medium was used for nitrite assessment whereas cells were lysed in 200 mM NaOH and protein content evaluated by Bradford's method. Results are expressed as  $\mu\text{mol}$  of nitrites/  $\mu\text{g}$  of proteins; data are means  $\pm$  SEM (n=5). \*\*\* P < 0.001 vs Control; §§ P<0.01 vs TII.

Figure 8. Effect of mTOR inhibitors on astrocytes. Rat cortical astrocytes were incubated in regular medium (Control) or medium activated with TII. As indicated, cells were co-incubated with RAD (A) and RAPA (B), within 0.01-10 nM range. After 48 h, NO production was assessed indirectly by measurement of nitrite accumulation in the incubation medium. Data are expressed as Means  $\pm$  SEM of 5-10 replicates per each group. \*\*\*, P<0.001 vs Control; one-way ANOVA followed by Bonferroni's post test. (C) Astrocytes were activated with TII for 48h and mTOR inhibitors were added at the beginning of each experiment, as indicated. Cells were incubated with MTS for 2 h after which the absorbance was measured at 490 nm. \* P<0.05 vs Control.

## References

1. Skaper SD. The brain as a target for inflammatory processes and neuroprotective strategies. *Ann N Y Acad Sci* 2007;1122:23-34.

2. Pittock SJ, Lucchinetti CF. The pathology of MS: new insights and potential clinical applications. *Neurologist* 2007;13:45-56.
3. Gay F. Activated microglia in primary MS lesions: defenders or aggressors?. *Int MS J* 2007;14(3):78-83.
4. Pannu R, Singh I. Pharmacological strategies for the regulation of inducible nitric oxide synthase: neurodegenerative versus neuroprotective mechanisms. *Neurochem Int* 2006;49:170-82.
5. Bagasra O, Michaels FH, Zheng YM, Bobroski LE, Spitsin SV, Fu ZF, Tawadros R, and Koprowski H. Activation of the inducible form of nitric oxide synthase in the brains of patients with multiple sclerosis. *Proc Natl Acad Sci USA* 1995;92:12041-5.
6. Zhao W, Tilton RG, Corbett JA, McDaniel ML, Misko TP, Williamson JR, Cross AH, and Hickey WF. Experimental allergic encephalomyelitis in the rat is inhibited by aminoguanidine, an inhibitor of nitric oxide synthase. *J Neuroimmunol* 1996;64:123-33.
7. Hooper DC, Bagasra O, Marini JC, Zborek A, Ohnishi ST, Kean R, Champion JM, Sarker AB, Bobroski L, Farber JL, Akaike T, Maeda H, and Koprowski H. Prevention of experimental allergic encephalomyelitis by targeting nitric oxide and peroxynitrite:

- 1  
2  
3 implications for the treatment of multiple sclerosis. *Proc Natl Acad Sci USA*  
4  
5 1997;94:2528-33.  
6  
7  
8  
9
- 10 8. Ding M, Zhang M, Wong JL, Rogers NE, Ignarro LJ, and Voskuhl RR. Antisense  
11 knockdown of inducible nitric oxide synthase inhibits induction of experimental  
12 autoimmune encephalomyelitis in SJL/J mice. *J Immunol* 1998; 160:2560-4.  
13  
14  
15  
16  
17  
18
- 19 9. Dalton DK, Wittmer S. Nitric-oxide-dependent and independent mechanisms of  
20 protection from CNS inflammation during Th1-mediated autoimmunity: evidence  
21 from EAE in iNOS KO mice. *J Neuroimmunol* 2005;160:110-21.  
22  
23  
24  
25  
26  
27
- 28 10. Zettl UK, Mix E, Zielasek J, Stangel M, Hartung HP, Gold R. Apoptosis of  
29 myelin-reactive T cells induced by reactive oxygen and nitrogen intermediates in vitro.  
30 *Cell Immunol* 1997;178:1-8.  
31  
32  
33  
34  
35  
36
- 37 11. Chan A, Hummel V, Weilbach FX, Kieseier BC, Gold R. Phagocytosis of  
38 apoptotic inflammatory cells downregulates microglial chemoattractive function and  
39 migration of encephalitogenic T cells. *J Neurosci Res* 2006; 84:1217-24.  
40  
41  
42  
43  
44  
45
- 46 12. Sharief MK, Matthews H, Noori MA. Expression ratios of the Bcl-2 family  
47 proteins and disease activity in multiple sclerosis. *J Neuroimmunol* 2003;134:158-65.  
48  
49  
50  
51  
52  
53  
54  
55  
56  
57  
58  
59  
60  
61  
62  
63  
64  
65

- 1  
2  
3 13. Wullschleger S, Loewith R, Hall MN. TOR signaling in growth and metabolism.  
4  
5 Cell 2006;124:471-84.  
6  
7  
8  
9
- 10 14. Battaglia M, Stabilini A, Roncarolo MG. Rapamycin selectively expands  
11  
12 CD4+CD25+FoxP3+ regulatory T cells. Blood 2005;105:4743-8.  
13  
14  
15  
16
- 17 15. Battaglia M, Stabilini A, Migliavacca B, Horejs-Hoeck J, Kaupper T, Roncarolo  
18  
19 MG. Rapamycin promotes expansion of functional CD4<sup>+</sup>CD25<sup>+</sup>FOXP3<sup>+</sup> regulatory T  
20  
21 cells of both healthy subjects and type 1 diabetic patients. J Immunol 2006;177:8338-  
22  
23 47.  
24  
25  
26  
27
- 28 16. Mondino A, Mueller DL. mTOR at the crossroads of T cell proliferation and  
29  
30 tolerance. Semin Immunol 2007;19:162-72.  
31  
32  
33  
34  
35
- 36 17. Jozwiak J, Jozwiak S, and Oldak M. Molecular activity of sirolimus and its  
37  
38 possible application in tuberous sclerosis treatment. Med Res Rev 2006; 26: 160-180.  
39  
40  
41  
42
- 43 18. Game DS, Hernandez-Fuentes MP, and Lechler RI. Everolimus and basiliximab  
44  
45 permit suppression by human CD4+CD25+ cells in vitro. Am J Transplant 2005; 5:  
46  
47 454-64.  
48  
49  
50  
51
- 52 19. Weichhart T, Säemann MD. The multiple facets of mTOR in immunity. Trends  
53  
54 Immunol 2009 Apr 8 [Epub ahead of print].  
55  
56  
57  
58  
59  
60  
61  
62  
63  
64  
65

- 1  
2  
3  
4  
5 20. Weichhart T, Costantino G, Poglitsch M, Rosner M, Zeyda M, Stuhlmeier KM,  
6  
7 Kolbe T, Stulnig TM, Hörl WH, Hengstschläger M, Müller M, Säemann MD. The  
8  
9 TSC-mTOR signaling pathway regulates the innate inflammatory response. *Immunity*  
10  
11 2008;29:565-77.  
12  
13  
14  
15  
16  
17 21. Thomson AW, Turnquist HR, Raimondi G. Immunoregulatory functions of  
18  
19 mTOR inhibition. *Nat Rev Immunol* 2009;9:324-37.  
20  
21  
22  
23  
24 22. Monti P, Mercuri A, Leone BE, Valerio DC, Allavena P, Piemonti L. Rapamycin  
25  
26 impairs antigen uptake of human dendritic cells. *Transplantation*. 2003;75:137-45.  
27  
28  
29  
30  
31 23. Fischer R, Turnquist HR, Taner T, Thomson AW. Use of rapamycin in the  
32  
33 induction of tolerogenic dendritic cells. *Handb Exp Pharmacol* 2009;188:215-32.  
34  
35  
36  
37  
38 24. Weinstein SL, Finn AJ, Davé SH, Meng F, Lowell CA, Sanghera JS, DeFranco  
39  
40 AL. Phosphatidylinositol 3-kinase and mTOR mediate lipopolysaccharide-stimulated  
41  
42 nitric oxide production in macrophages via interferon-beta. *J Leukoc Biol* 2000;  
43  
44 67:405-14.  
45  
46  
47  
48  
49  
50 25. Schmitz F, Heit A, Dreher S, Eisenächer K, Mages J, Haas T, Krug A, Janssen  
51  
52 KP, Kirschning CJ, Wagner H. Mammalian target of rapamycin (mTOR) orchestrates  
53  
54 the defense program of innate immune cells. *Eur J Immunol* 2008;38:2981-92.  
55  
56  
57  
58  
59  
60  
61  
62  
63  
64  
65

- 1  
2  
3  
4  
5 26. Chong ZZ, Li F, Maiese K. The pro-survival pathways of mTOR and protein  
6  
7 kinase B target glycogen synthase kinase-3 $\beta$  and nuclear factor- $\kappa$ B to foster  
8  
9 endogenous microglial cell protection. *Int J Mol Med*. 2007;19:263-72.  
10  
11  
12  
13  
14 27. Lu DY, Liou HC, Tang CH, Fu WM. Hypoxia-induced iNOS expression in  
15  
16 microglia is regulated by the PI3-kinase/Akt/mTOR signaling pathway and activation  
17  
18 of hypoxia inducible factor-1 $\alpha$ . *Biochem Pharmacol* 2006;72:992-1000.  
19  
20  
21  
22  
23 28. Chiang GG, Abraham RT. Phosphorylation of mammalian target of rapamycin  
24  
25 (mTOR) at Ser-2448 is mediated by p70S6 kinase. *J Biol Chem* 2005;280:25485-90.  
26  
27  
28  
29  
30 29. Dello Russo C, Boullerne AI, Gavriluk V, Feinstein DL. Inhibition of microglial  
31  
32 inflammatory responses by norepinephrine: effects on nitric oxide and interleukin-  
33  
34 1 $\beta$  production. *J Neuroinflammation*. 2004;1:9.  
35  
36  
37  
38  
39 30. Vairano M, Dello Russo C, Pozzoli G, Battaglia A, Scambia G, Tringali G, Aloe-  
40  
41 Spiriti MA, Preziosi P, Navarra P. Erythropoietin exerts anti-apoptotic effects on rat  
42  
43 microglial cells in vitro. *Eur J Neurosci* 2002;16:584-92.  
44  
45  
46  
47  
48  
49 31. Green LC, Wagner DA, Glogowski J, Skipper PL, Wishnok JS, Tannenbaum SR.  
50  
51 Analysis of nitrate, nitrite, and [15N]nitrate in biological fluids. *Anal Biochem* 1982;  
52  
53 126:131-8.  
54  
55  
56  
57  
58  
59  
60  
61  
62  
63  
64  
65



- 1  
2  
3  
4  
5 32. Tringali G, Pozzoli G, Vairano M, Mores N, Preziosi P, Navarra P: Interleukin-18  
6  
7 displays effects opposite to those of interleukin-1 in the regulation of neuroendocrine  
8  
9 stress axis. *J Neuroimmunol* 2005;160:61-7.  
10  
11  
12  
13  
14 33. Livak KJ, Schmittgen TD: Analysis of relative gene expression data using real-  
15  
16 time quantitative PCR and the 2(-Delta Delta C(T)) Method *Methods* 2001;25:402-8.  
17  
18  
19  
20  
21 34. Galea E, Feinstein DL, Reis DJ. Induction of calcium-independent nitric oxide  
22  
23 synthase activity in primary rat glial cultures. *Proc Natl Acad Sci U S A*  
24  
25 1992;89:10945-9.  
26  
27  
28  
29  
30 35. Yang CS, Song CH, Lee JS, Jung SB, Oh JH, Park J, Kim HJ, Park JK, Paik TH,  
31  
32 Jo EK. Intracellular network of phosphatidylinositol 3-kinase, mammalian target of the  
33  
34 rapamycin/70 kDa ribosomal S6 kinase 1, and mitogen-activated protein kinases  
35  
36 pathways for regulating mycobacteria-induced IL-23 expression in human  
37  
38  
39  
40  
41  
42  
43  
44  
45 36. Dos Santos Mendes S, Candi A, Vansteenbrugge M, Pignon MR, Bult H,  
46  
47 Boudjeltia KZ, Munaut C, Raes M. Microarray analyses of the effects of NF-kappaB  
48  
49 or PI3K pathway inhibitors on the LPS-induced gene expression profile in RAW264.7  
50  
51  
52  
53  
54  
55  
56  
57  
58  
59  
60  
61  
62  
63  
64  
65

37. Minhajuddin M, Bijli KM, Fazal F, Sassano A, Nakayama KI, Hay N, Platanias LC, Rahman A. Protein kinase C-delta and phosphatidylinositol 3-kinase/Akt activate mammalian target of rapamycin to modulate NF-kappaB activation and intercellular adhesion molecule-1 (ICAM-1) expression in endothelial cells. *J Biol Chem* 2009; 284:4052-61.
38. Lorne E, Zhao X, Zmijewski JW, Liu G, Park YJ, Tsuruta Y, Abraham E. Participation of mTOR Complex 1 in TLR2 and TLR4 Induced Neutrophil Activation and Acute Lung Injury. *Am J Respir Cell Mol Biol* 2009 Jan 8 [Epub ahead of print].
39. Glantschnig H, Fisher JE, Wesolowski G, Rodan GA, Reszka AA. M-CSF, TNFalpha and RANK ligand promote osteoclast survival by signaling through mTOR/S6 kinase. *Cell Death Differ* 2003; 10:1165-77.
40. Solà-Vilà D, Camacho M, Solà R, Soler M, Diaz JM, Vila L. IL-1beta induces VEGF, independently of PGE2 induction, mainly through the PI3-K/mTOR pathway in renal mesangial cells. *Kidney Int* 2006;70:1935-41.
41. Schreml S, Lehle K, Birnbaum DE, Preuner JG. mTOR-inhibitors simultaneously inhibit proliferation and basal IL-6 synthesis of human coronary artery endothelial cells. *V Int Immunopharmacol*. 2007;7:781-90.

- 1  
2  
3 42. Ozes ON, Akca H, Mayo LD, Gustin JA, Maehama T, Dixon JE, Donner DB. A  
4  
5 phosphatidylinositol 3-kinase/Akt/mTOR pathway mediates and PTEN antagonizes  
6  
7 tumor necrosis factor inhibition of insulin signaling through insulin receptor substrate-  
8  
9 1. Proc Natl Acad Sci U S A 2001;98:4640-5.  
10  
11  
12  
13  
14  
15 43. Lee DF, Kuo HP, Chen CT, Hsu JM, Chou CK, Wei Y, Sun HL, Li LY, Ping B,  
16  
17 Huang WC, He X, Hung JY, Lai CC, Ding Q, Su JL, Yang JY, Sahin AA, Hortobagyi  
18  
19 GN, Tsai FJ, Tsai CH, Hung MC. IKK beta suppression of TSC1 links inflammation  
20  
21 and tumor angiogenesis via the mTOR pathway. Cell 2007;130:440-55.  
22  
23  
24  
25  
26  
27 44. Ma XM, Blenis J. Molecular mechanisms of mTOR-mediated translational  
28  
29 control. Nat Rev Mol Cell Biol 2009;10:307-18.  
30  
31  
32  
33  
34 45. Hartford CM, Ratain MJ. Rapamycin: something old, something new, sometimes  
35  
36 borrowed and now renewed. Clin Pharmacol Ther 2007; 82: 381-388.  
37  
38  
39  
40  
41 46. Croons V, Martinet W, Herman AG, Timmermans JP, De Meyer GR. Selective  
42  
43 clearance of macrophages in atherosclerotic plaques by the protein synthesis inhibitor  
44  
45 cycloheximide. J Pharmacol Exp Ther 2007;320:986-93.  
46  
47  
48  
49  
50 47. Woltman AM, van der Kooij SW, Coffey PJ, Offringa R, Daha MR, van Kooten  
51  
52 C. Rapamycin specifically interferes with GM-CSF signaling in human dendritic cells,  
53  
54 leading to apoptosis via increased p27KIP1 expression. Blood 2003;101:1439-45.  
55  
56  
57  
58  
59  
60  
61  
62  
63  
64  
65

- 1  
2  
3  
4  
5 48. Erlich S, Alexandrovich A, Shohami E, Pinkas-Kramarski R. Rapamycin is a  
6  
7 neuroprotective treatment for traumatic brain injury. *Neurobiol Dis.* 2007;26:86-93.  
8  
9  
10  
11  
12 49. Codeluppi S, Svensson CI, Hefferan MP, Valencia F, Silldorff MD, Oshiro M,  
13  
14 Marsala M, Pasquale EB. The Rheb-mTOR pathway is upregulated in reactive  
15  
16 astrocytes of the injured spinal cord. *J Neurosci* 2009;29:1093-104.  
17  
18  
19  
20  
21  
22  
23  
24  
25  
26  
27  
28  
29  
30  
31  
32  
33  
34  
35  
36  
37  
38  
39  
40  
41  
42  
43  
44  
45  
46  
47  
48  
49  
50  
51  
52  
53  
54  
55  
56  
57  
58  
59  
60  
61  
62  
63  
64  
65

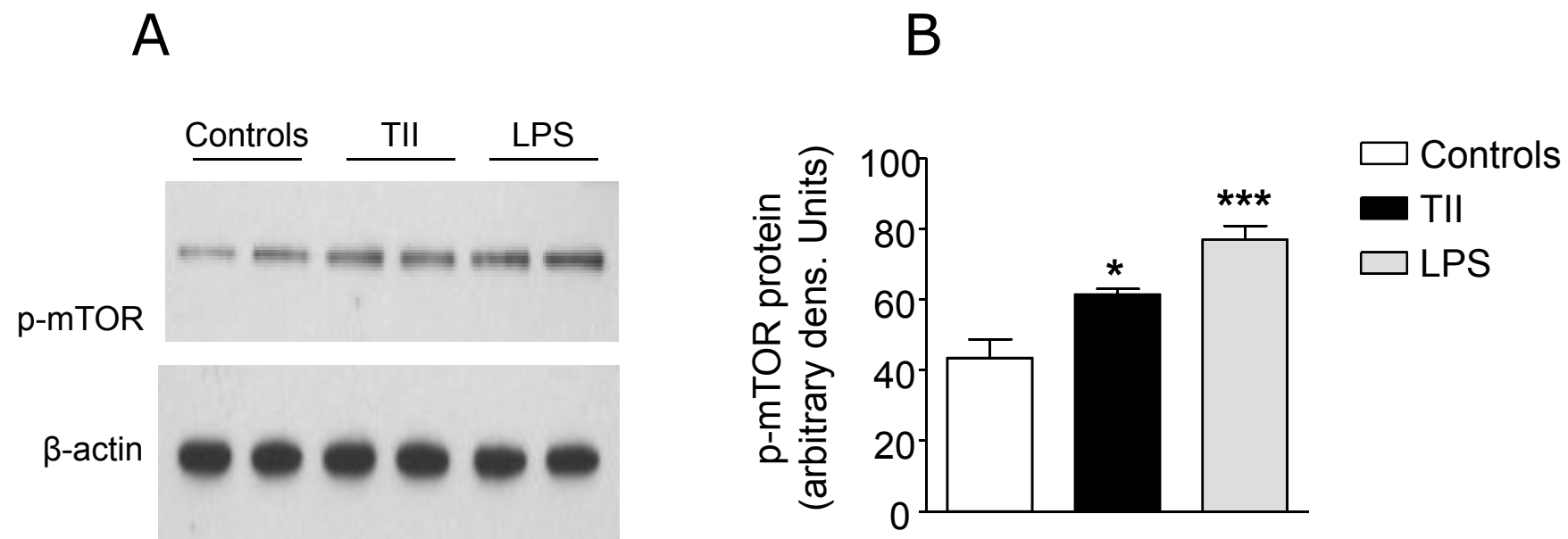
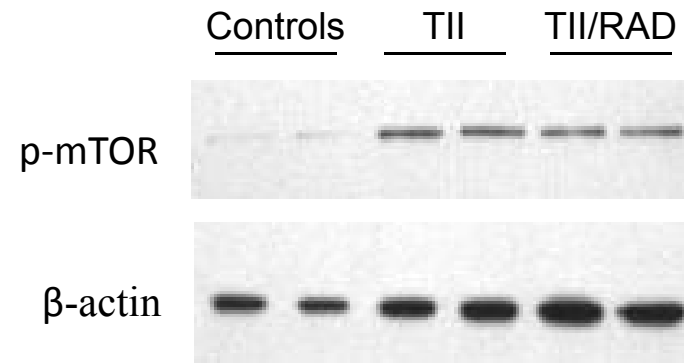


Figure 1

A



B

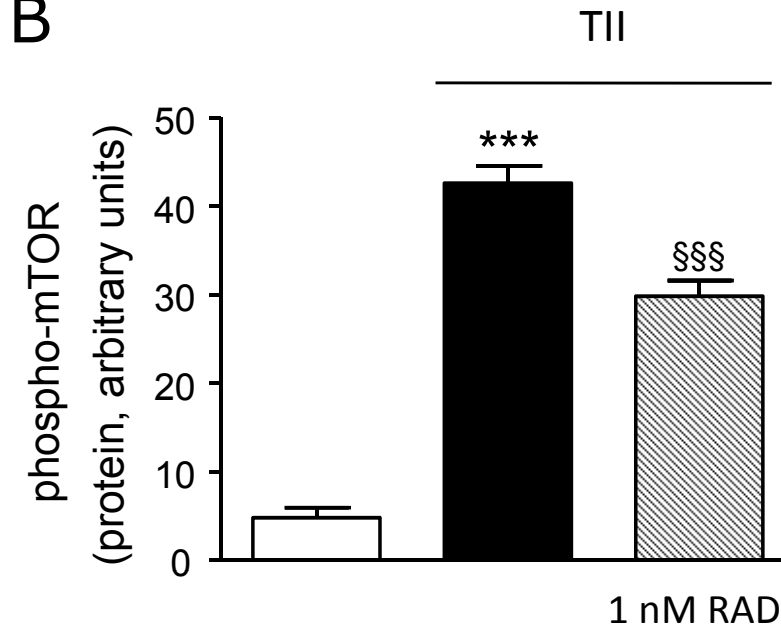


Figure 2

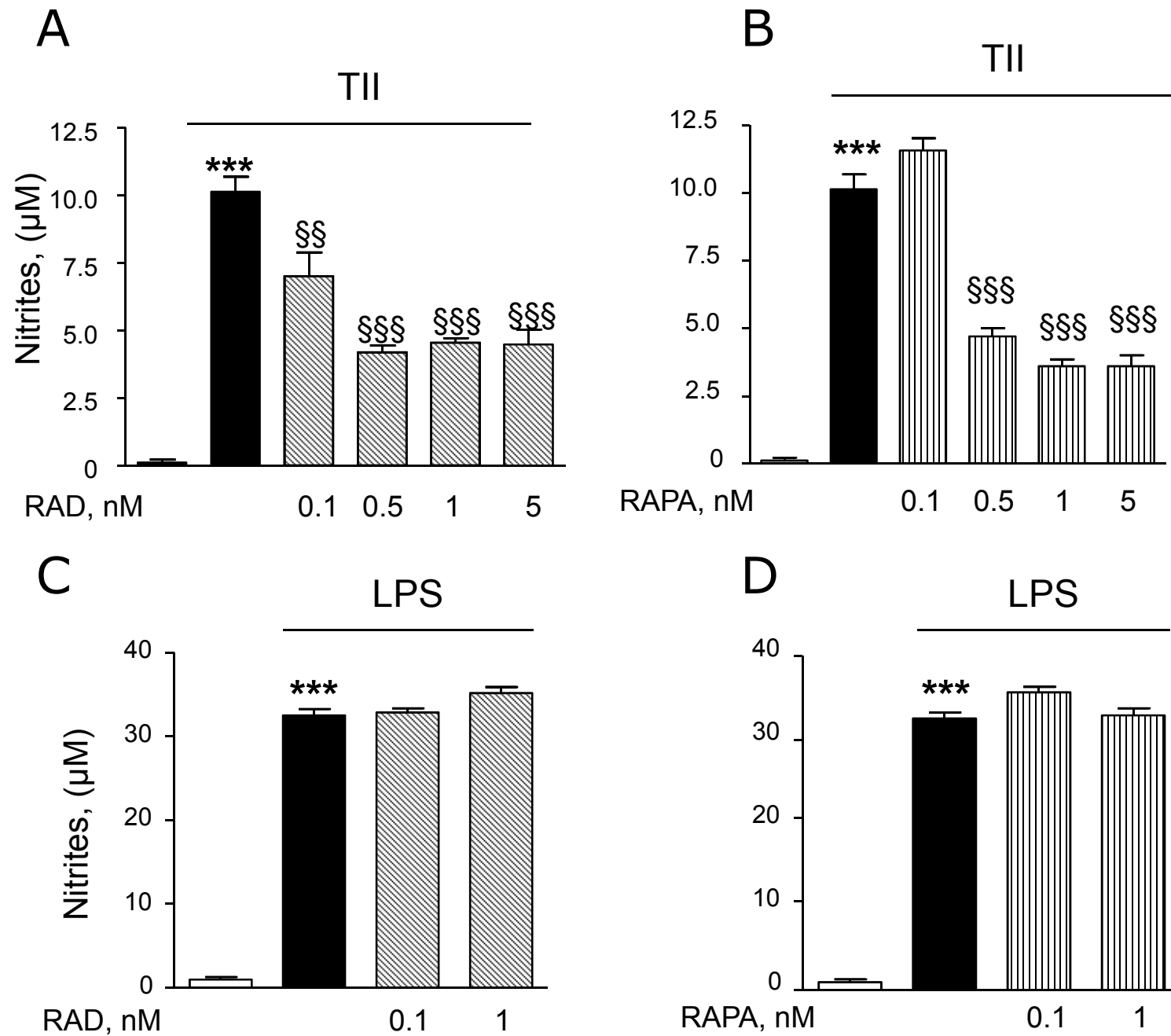


Figure 3

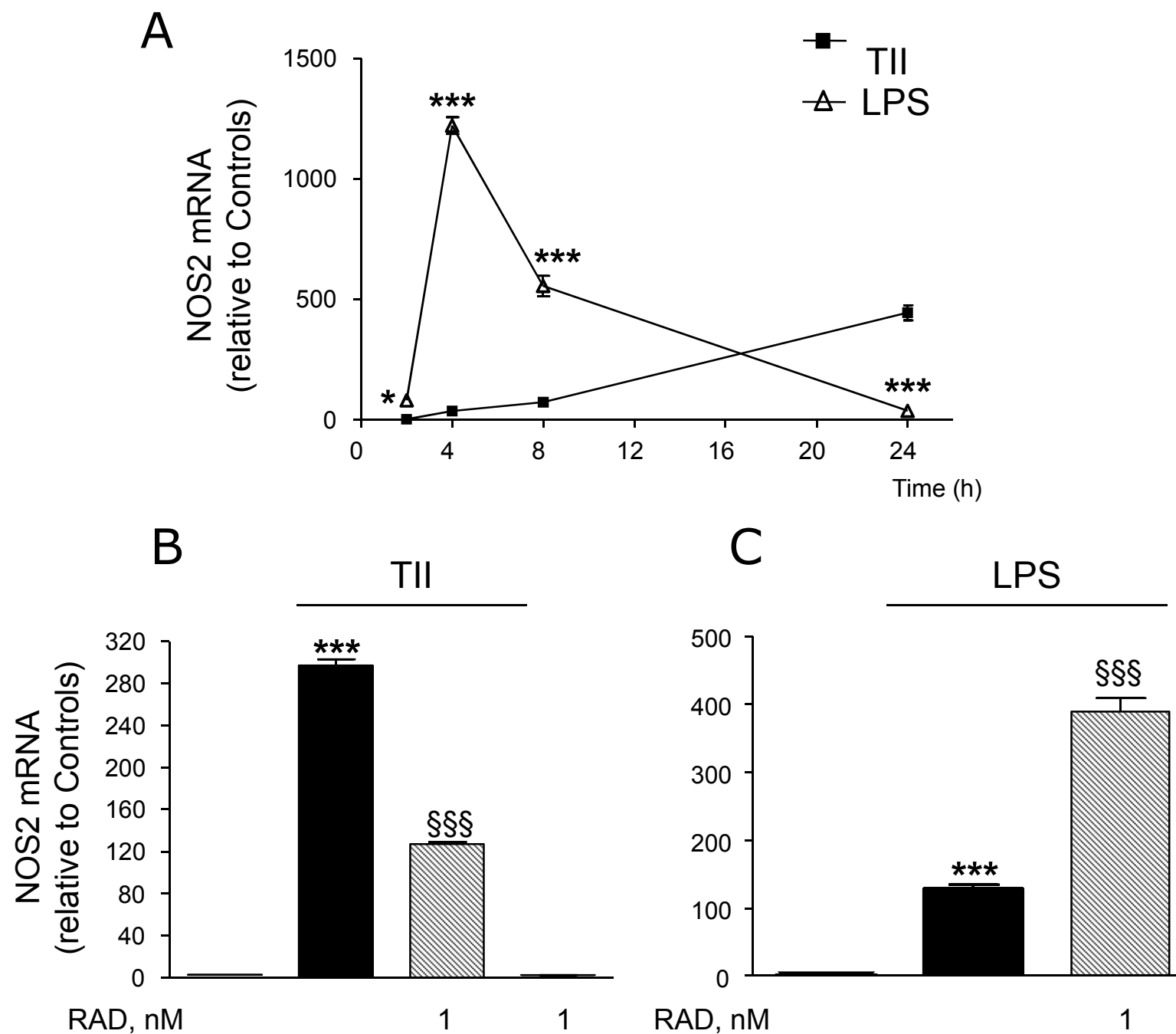


Figure 4



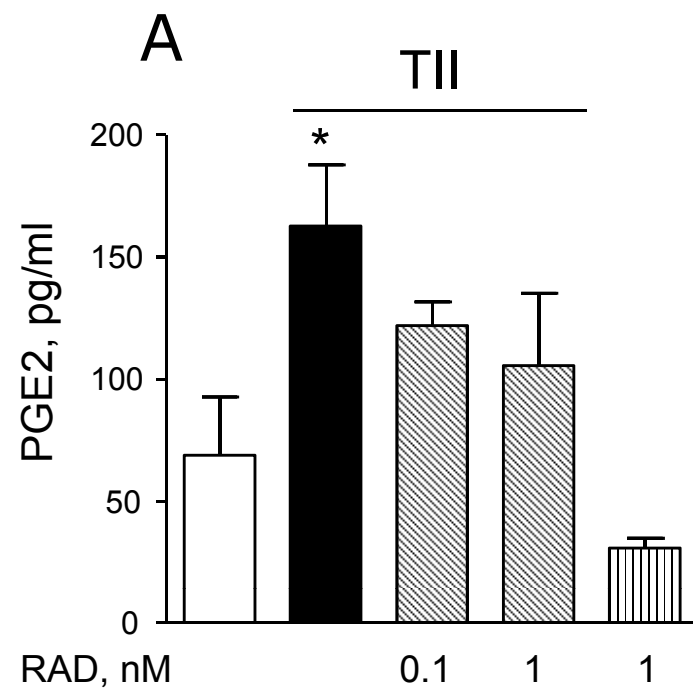


Figure 5

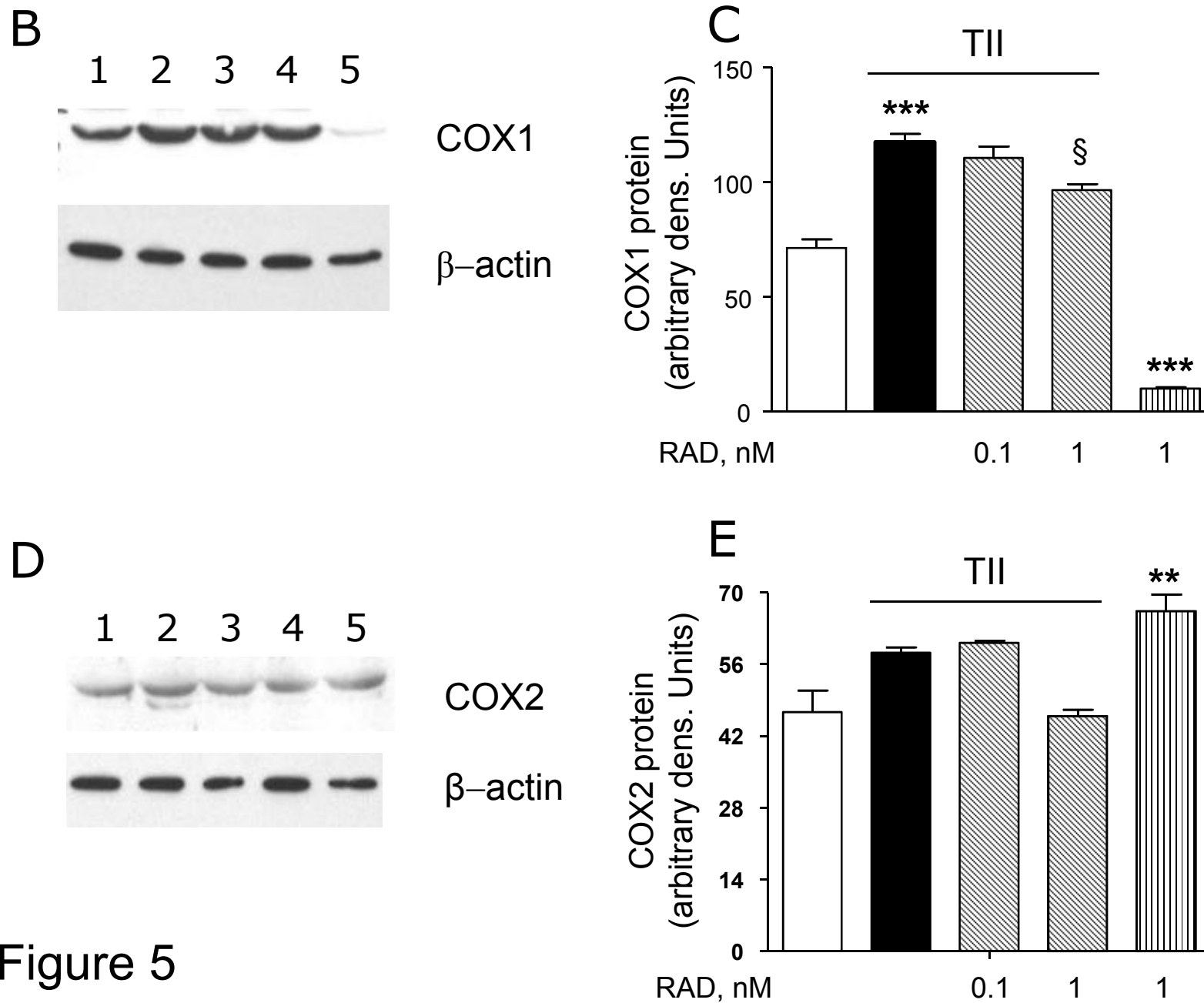


Figure 5

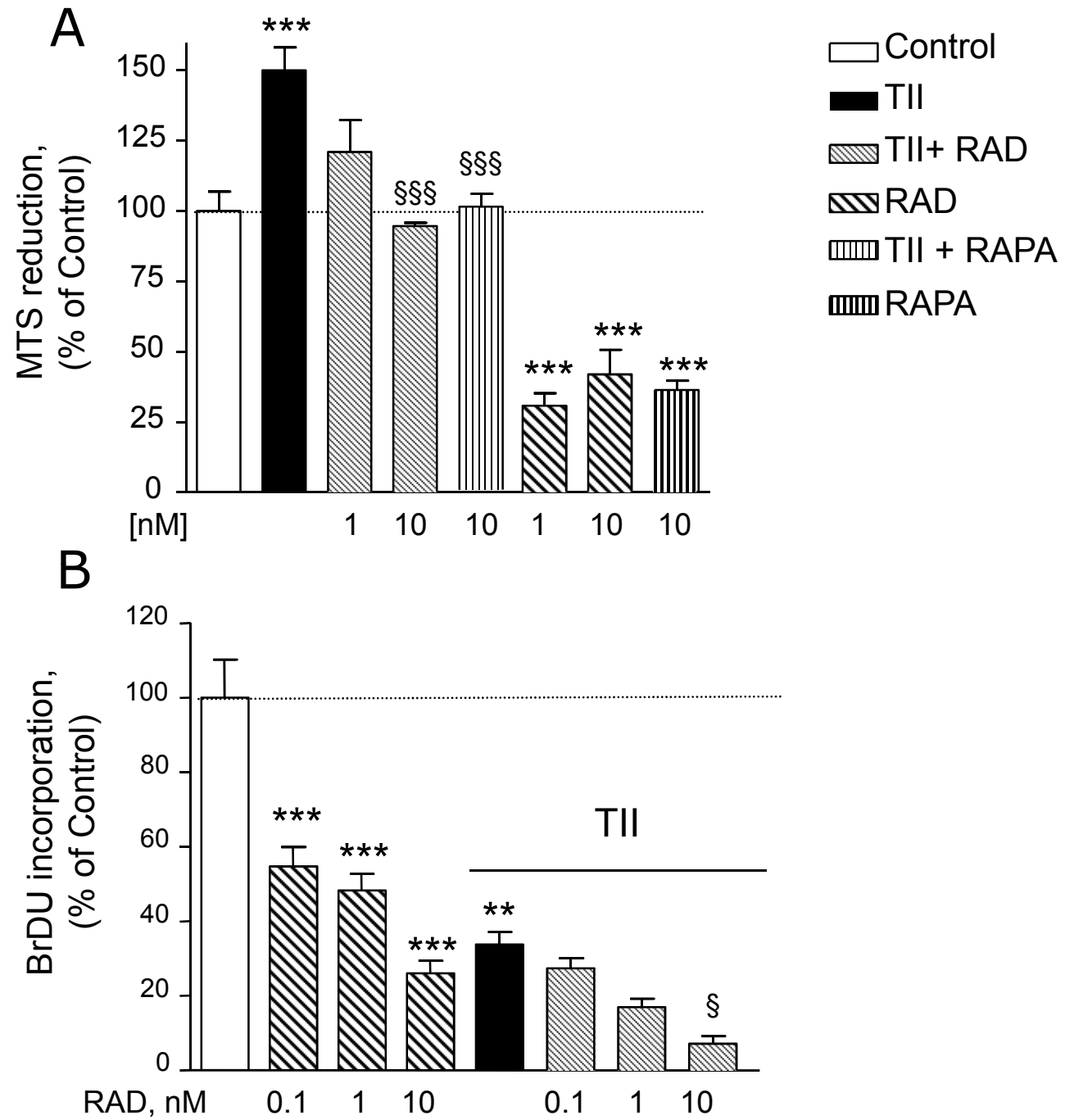


Figure 6

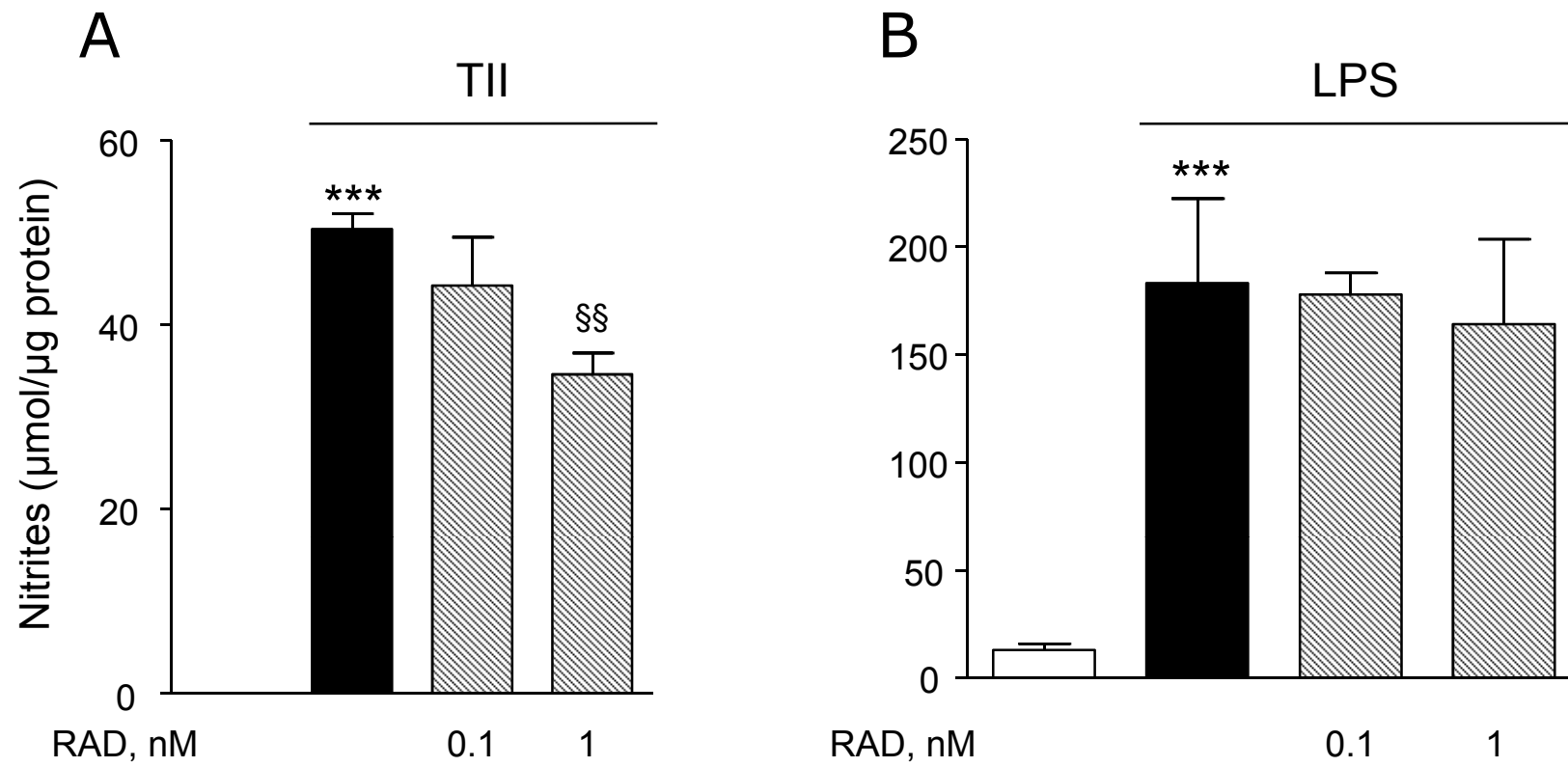


Figure 7

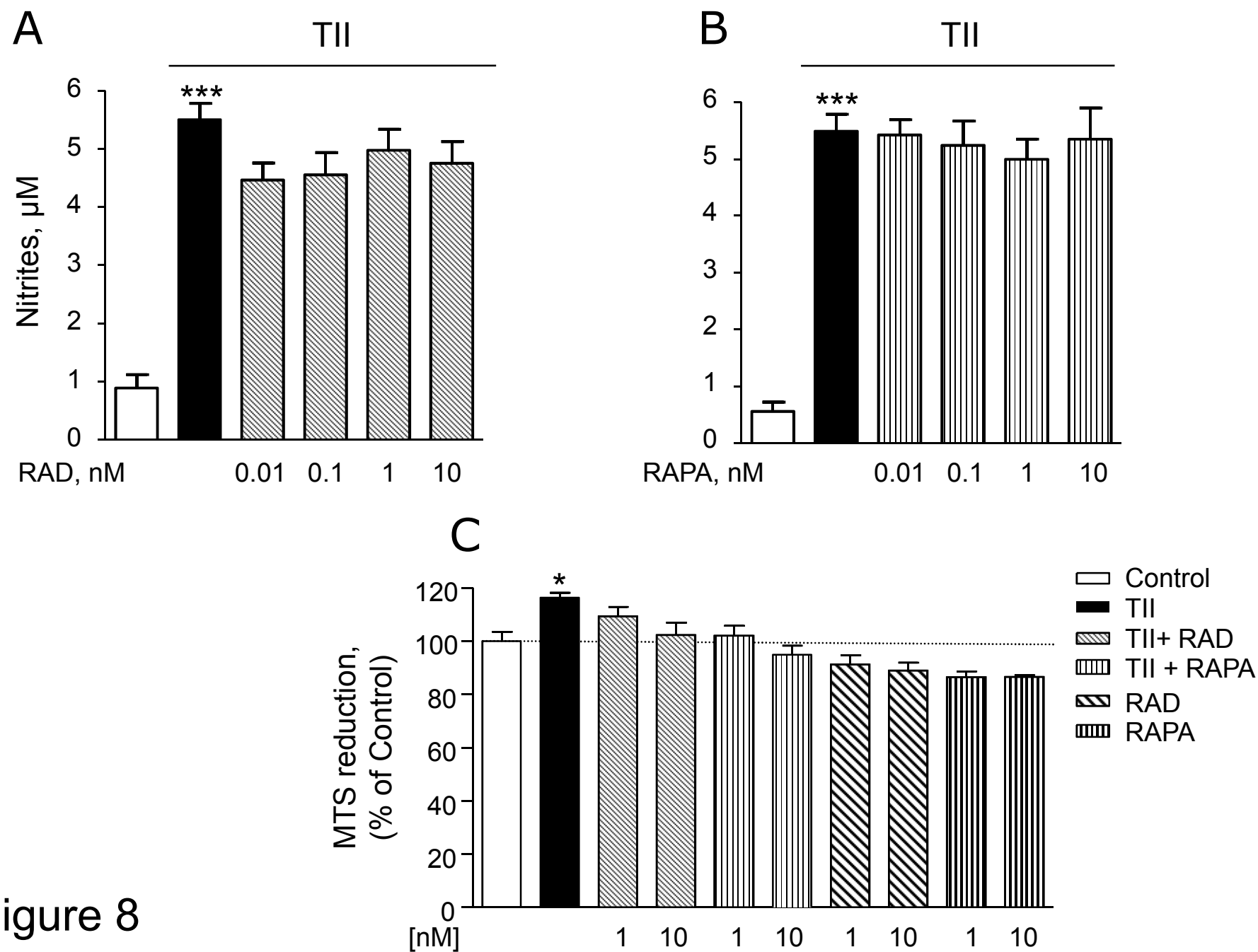


Figure 8